Ultrastructural and Morphometric Studies of Delta Cells in Pancreatic Islets from C57BL/Ks Diabetes Mice

E. H. Leiter, D. A. Gapp, J. J. Eppig, and D. L. Coleman

The Jackson Laboratory, Bar Harbor, Maine, USA

Summary. An ultrastructural and immunocytochemical study was undertaken to elucidate the temporal and quantitative aspects of the changes occurring in the delta cells in the pancreatic islets of C57BL/KsJ *db/db* (diabetes) mice. Electron microscopy revealed that prior to the major topographical redistribution of delta cells from their peripheral location to the islet interior, long delta cell filopodial extensions penetrated into the islet, greatly increasing the area of surface contact between delta cells and hypersecretory beta cells. Coincident with delta cell redistribution in islets of 8 to 10 week diabetes mice, the mean number of delta cells per islet had increased significantly. In contrast, their volume density had decreased, indicating incomplete compensation for beta cell hyperplasia which had commenced approximately 4 weeks earlier. In the 14 week mutants, numbers of delta cells per islet and islet volume reached maximum values while delta cell volume density had been restored to a control level. Delta cell volume density exhibited a 2-fold increase in the mutants at 20 weeks that coincided with massive beta cell necrosis. However, a decline in the number of delta cells per islet (173.6 ± 20.9 at 14 weeks versus 91.2 ± 9.5 at 20 weeks) suggests that islet degeneration in terminal stages of the syndrome also includes some loss of these cells.

Key words: Diabetes mice, pancreatic islets, D cell, somatostatin, B cell, A cell, PP cell, electron microscopy, morphometric analysis.

The widely-distributed tetradecapeptide somatostatin is a potent inhibitor of secretory function of pancreatic insulin-producing beta (B) cells, glucagon-producing (A) cells, and pancreatic polypeptide (PP) producing cells both in vivo [1, 16, 20, 22] and in vitro [8, 10, 30]. The localization of somatostatin within the secretory granules of the delta (D) cell in the islets of Langerhans [6, 7, 11, 25] raises the possibility that this cell type may be an important physiological regulator of normal A, B, and PP cell function. Orci and Unger [24] have speculated as to the nature of intra-islet "paracrine" relationships, noting that alterations in the intercellular relationships among pancreatic endocrine cells occur in laboratory rodents in hyperinsulinaemic and hypoinsulinaemic states.

Genetically diabetic *(db/db)* inbred mice have proved useful for the study of islet cell relationships since the *db* gene interaction with the inbred background results in different diabetic syndromes [3] with differing degrees of perturbation of islet composition and structure [2]. Thus, in C57BL/KsJ (BL/Ks) *db/db* mice which exhibit obesity, transient hyperinsulinaemia, hyperglycaemia, and ultimate necrosis and atrophy of the B cells [4, 18, 19] there is a decrease in B cell volume density coupled with an increase in A, D, and PP cell volume density and a concomitant loss in normal peripheral distribution of the non-B cells [2]. In contrast, in C57BL/6J (BL/6) *db/db* mice which are characterized by severe obesity, hyperinsulinaemia, mild hyperglycaemia and greatly enlarged B cell-rich islets, there is a decrease in A, D, and PP cell volume density and a minor perturbation of the peripheral position of these cell types [2].

Since the original ultrastructural study performed in the BL/Ks *db/db* islets during disease progression omitted a description of the timing and the nature of the topographical changes in the D cell population [19], the purpose of this study was to examine these changes by light and electron microscopy. Further,

the increase in volume density of D cells documented for the islets of old BL/Ks *db/db* mice [2] was only a relative measure of D cell abundance in the face of a declining islet volume due to B cell necrosis and atrophy. In order to determine whether an absolute increase in D cells occurs prior to the stage of B cell loss, we have undertaken a quantitative morphometric analysis of immunocytochemically-stained islets from mutant mice at three different stages of disease progression.

Materials and Methods

Inbred Mice

Diabetic BL/Ks mice between 4 and 20 weeks of age and their normal littermate controls were bred in our research colonies at the Jackson Laboratory and were fed *ad libitum* on diet 96W (Emory Morse Co., Old Guilford, Conn.) until sacrifice. Pre-weaning, non-obese *db/db* and littermate control mice were obtained from our colony in which the gene diabetes *(db)* was maintained in linkage with the misty *(m)* colour marker gene [5].

Electron Microscopy

Pancreatic islets for ultrastructural observation were obtained from tribromoethanol-anaesthetized mice (5 mg/10 g body weight) by intraventricular perfusion for 30 s to 1 min of Ringer's-lactate (pH 7.4) solution containing procaine-HCl (0.1 g/100 ml), heparin (100 units/ml), and polyvinylpyrrolidone (2 g/100 ml) (Sigma, St. Louis, Mo., 40,000 mol.wt.) at a pressure of between 80–100 mm Hg. Immediately following the rinse, fixative [2% glutaraldehyde/1% formaldehyde buffered in 0.1 mol/l cacodylate, pH 7.2, and also containing 0.2 mmol/l $CaCl_2$ and 2% polyvinylpyrrolidone (PVP)] was perfused at the same pressure for 5–10 min. The perfused pancreas was then excised, placed into the fixative (without PVP) in a Petri dish, and islets visible through a dissecting microscope were hand-microdissected free of the exocrine parenchyma and post-fixed for 2 h. In some instances, islets were also isolated from freshly-minced pancreas by vigorous manual shaking for 10–12 min at 37°C in a collagenase solution (Worthington, Freehold, N. J., type IV, 300 units/mg, 1 mg/ml in Hanks' balanced salt solution modified to contain 15 mmol/l Hepes buffer, pH 7.4). Following two washes in modified Hanks' solution, islets visible in the collagenase treated material were stripped free of contaminating tissue and were placed in fixative for 2 h. After fixation, islets were washed in the cacodylate buffer and were postfixed in 1 g/100 ml osmium tetroxide for 1 h, stained in 0.5 g/100 ml uranyl acetate in 0.1 mol/l sodium acetate for 1 h, dehydrated through a graded series of ethanol, and embedded in Epon 812. Thin sections were stained with uranyl acetate and lead citrate and examined in a Hitachi HU-11C electron microscope at an operating voltage of 75 KV.

Immunohistochemistry

Pancreases from 26 control and 36 diabetic mice were examined to determine the distribution of D cells within the islets and to establish the chronology of D cell redistribution during the development of diabetes. Hydrated 5 μ sections of Bouin's-fixed, paraffin-embedded tissue were stained for somatostatin by the peroxidase

anti-peroxidase method [29]. Briefly, following a 30 min preincubation with 3 ml/100 ml normal goat serum, the sections were incubated for 36–48 h at 4°C with rabbit anti-somatostatin serum (1:10,000, lot No. 101, kindly provided by Dr. A. Arimura) followed by sequential incubation with goat antirabbit gamma globulin serum (1:50, Polysciences, Inc., Warrington, Pa.) and rabbit peroxidase antiperoxidase (PAP, 1:50, Polysciences, Inc., Warrington, Pa.) for 30 min each at room temperature. (All antisera were prepared in 5 mmol/l tris/0.15 mol/l NaCl/1 ml/100 ml normal goat serum, pH 7.6). The resulting immune complex was detected with 50 mg/100 ml diaminobenzidine · 4HCl/0.01 ml/ 100 ml H_2O_2 dissolved in 5 mmol/l tris, pH 7.6. The specificity of the staining procedure was shown in control experiments where all staining was eliminated using primary antiserum which had been preadsorbed with 8 μg/ml synthetic cyclic somatostatin (Beckman Instruments, Inc., Palo Alto, Calif.). A cells and PP cells were immunocytochemically stained in a similar manner employing rabbit antiglucagon serum (1:100,000, lot No. R-2, 10-2, a gift from Dr. W. Rhoten) and rabbit anti-bovine pancreatic polypeptide serum (1:30,000, lot No. 615R11-146-16, kindly provided by Dr. R. Chance), respectively.

Morphometric Analysis

Islets for analysis were chosen randomly and were not selected on the basis of size; at least 10 islets per animal were analyzed with 2 to 4 animals per genotype and per age group. The only criteria placed upon islets chosen for analysis were [1] that the islets chosen were completely circumscribed by the series of sections available, [2] that the immunocytochemical staining was applied uniformly over the slides represented, and]3] that the islet did not fuse with another islet. Islet area measurements obtained using the internally calibrated image analyzer were found to be in close agreement with values obtained by projecting microscopic images of serially sectioned islets onto tracing paper, the tracings then being analyzed by planimetry.

Individual islets in pancreases of mice from 8 to 10, 14, and 20 week age group were analyzed in their entirety through immunocytochemically-stained 5 μ serial sections. Total islet area and D cell area were quantified with an Optomax quantitative image analysis system (Optomax, Inc., Burlington, Mass.). The operation of this system has been previously described [12, 13]. PAP-stained "particles" (both whole D cells and isolated D cell cytoplasmic processes) detected by the image analyzer also were counted during the analysis. Since the nucleus of the D cell averaged about 10 μ in diameter and was usually seen to overlap into two consecutive 5 μ sections, the total number of nucleated D cells per islet (obtained by summing the counts for all the serial sections) was divided by 2 to correct for nuclear overlap. Individual D cell shapes in islets of control mice, and especially in those of diabetic mice, were highly irregular such that determination of a mean D cell diameter was not feasible. For each islet analyzed, islet volume, D cell number per islet, mean number of PAP-positive particles detected per islet section, the total D cell volume, and D cell volume density were calculated to assess the question of D cell hypertrophic and/or hyperplastic changes during diabetes.

Results

Light Microscopic Observations

Immunocytochemically stained D cells were localized to the peripheral region of the islet in normal mice of all ages (Fig. 1 a) and in diabetic mice up to approxi-
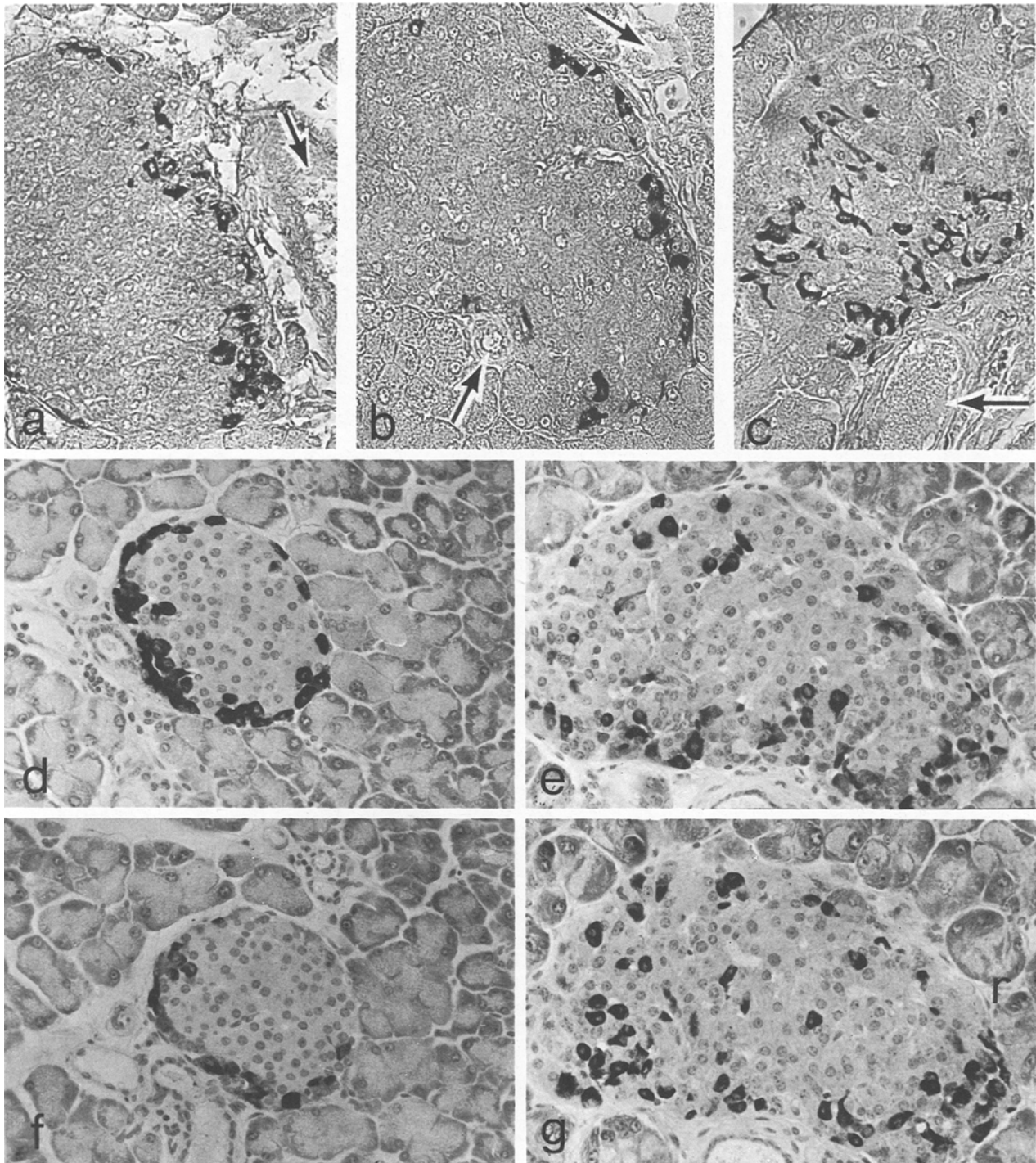
Fig. 1a–g. Immunocytochemical staining for somatostatin, glucagon, and pancreatic polypeptide in normal and diabetic islets. **a** Islet from a normal 11 week ♀ mouse showing D cell localized at the islet periphery and capped near a large blood vessel (arrow). **b** Islet from an 8 week ♀ *db/db* mouse exhibiting established hyperglycaemia but, as of yet, no D cell migration. Arrow indicates blood vessels. **c** Islet from an 11 week ♀ *db/db* mouse (littermate of a. above) demonstrating redistribution of D cells from peripheral location and away from the vasculature (arrow). **d** Islet from a normal 14 week ♀ mouse showing peripheral distribution of A cells. **e** Islet from a 14 week ♀ *db/db* mouse showing a hyperplastic islet stained for glucagon and showing an altered A cell distribution. **f–g** Semiadjacent 5 μ sections to those shown in panels d. and e. and stained for pancreatic polypeptide. An altered distribution of PP cells in the mutant islet (**g**) is seen as compared to control (**f**). **a–c**, × 250. **d–f**, haematoxylin counterstained, × 260
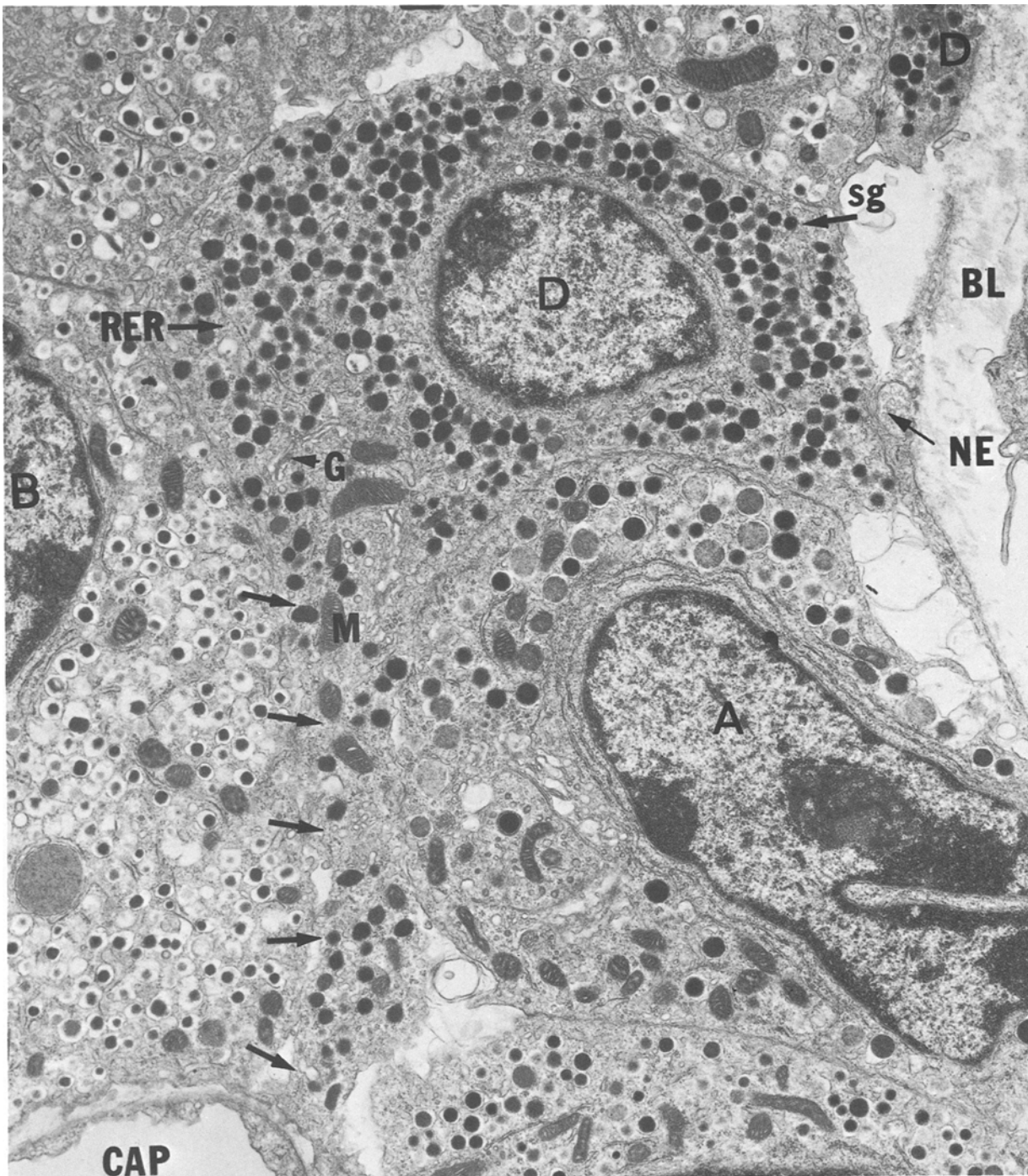
Fig. 2. Peripheral localization of D cells in islet of normal 12 week-old ♀ mouse. One of the D cells that borders on the periphery of the islet contacts an intra-islet capillary by means of a cytoplasmic process (arrow). Perfusion fixed, × 10,350. Common abbreviations used in this and the following electron micrographs: A: alpha cell – B: beta cell – BL: basal lamina – Cap.: capillary – D: delta cell – G: Golgi – M: mitochondria – NE: nerve ending – RER: rough endoplasmic reticulum – sg: secretory granule

mately 8–10 weeks of age (Fig. 1b). The D cells were not distributed uniformly around the heterocellular mantle layer; rather, they appeared oriented or "capped" at regions of the islet periphery adjacent to vascular and/or ductal structures (Fig. 1a, b), with only

occasional D cells being observed within the B cell core or in an "uncapped" position. The time of onset of perturbation of D cell topography in islets of diabetic mice varied with the individual but generally occurred between 8–10 weeks of age. This was
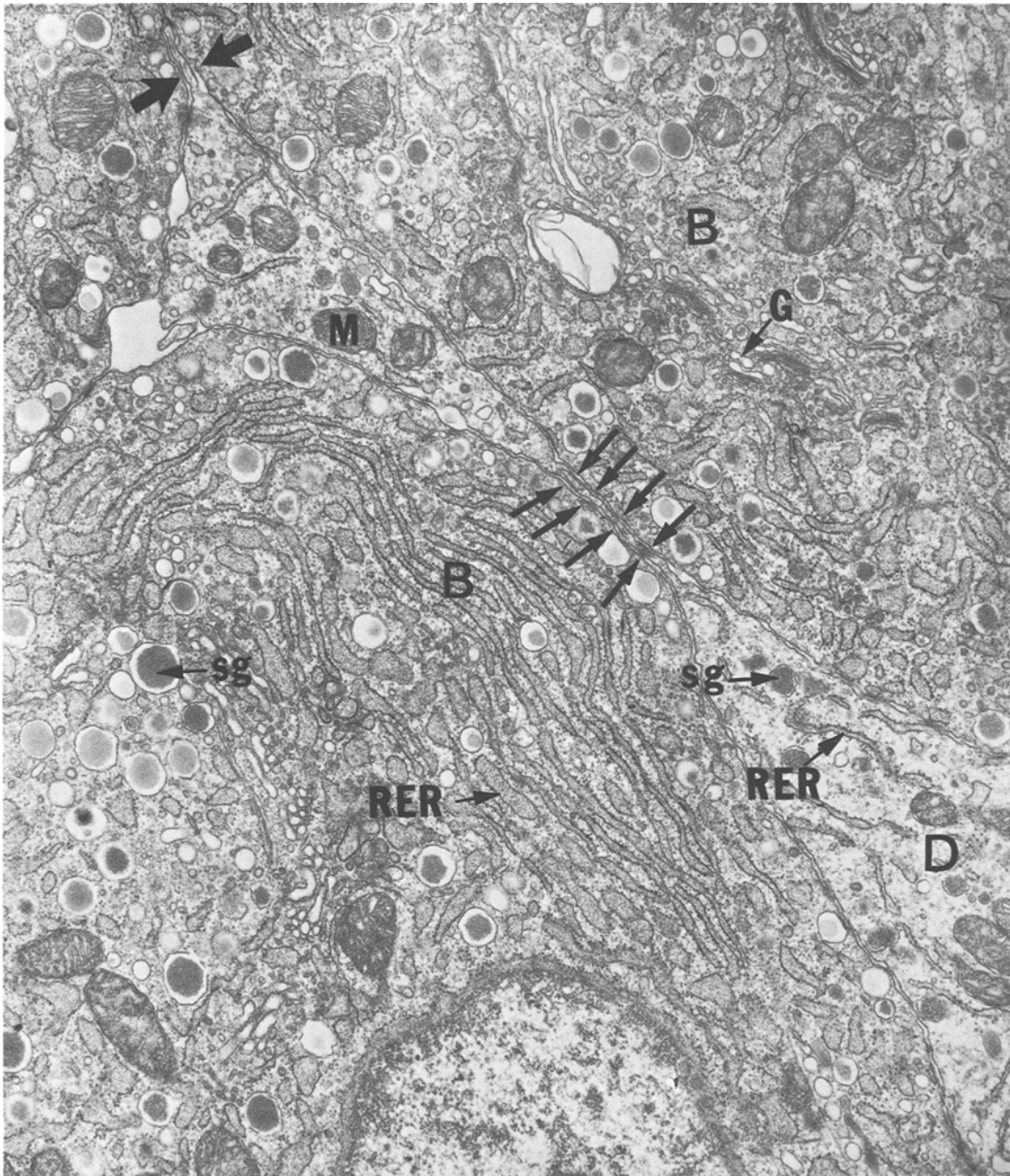
Fig. 3. D cell cytoplasmic process intercalating through the interstitial space between moderately degranulated B cells in the interior of a 7 week-old *db/db* islet. Large arrows denote a pseudopod; small arrows show a continuity in the D cell process as it insinuates between B cells. Perfusion fixed, × 16,500

characterized by alteration of D cell morphology and by penetration of D cell processes and later, by apparent migration of whole D cells into the B cell mass (Fig. 1c). Concomitant with these changes was an increase in the incidence observed of "uncapped" D cells (Fig. 1c). This redistribution phenomenon was not unique to the D cell population insofar as a similar change in A cell (Fig. 1d and e) and PP cell (Fig. 1f and g) topography was observed in islets of

mutant mice with established hyperglycaemia (10 weeks and older).

Ultrastructural Observations

D cells in normoglycaemic BL/Ks mice at all ages studied were generally found clustered at or near the periphery of the islets near capillaries (Fig. 2). Nuclei of D cells were usually positioned at one pole of the
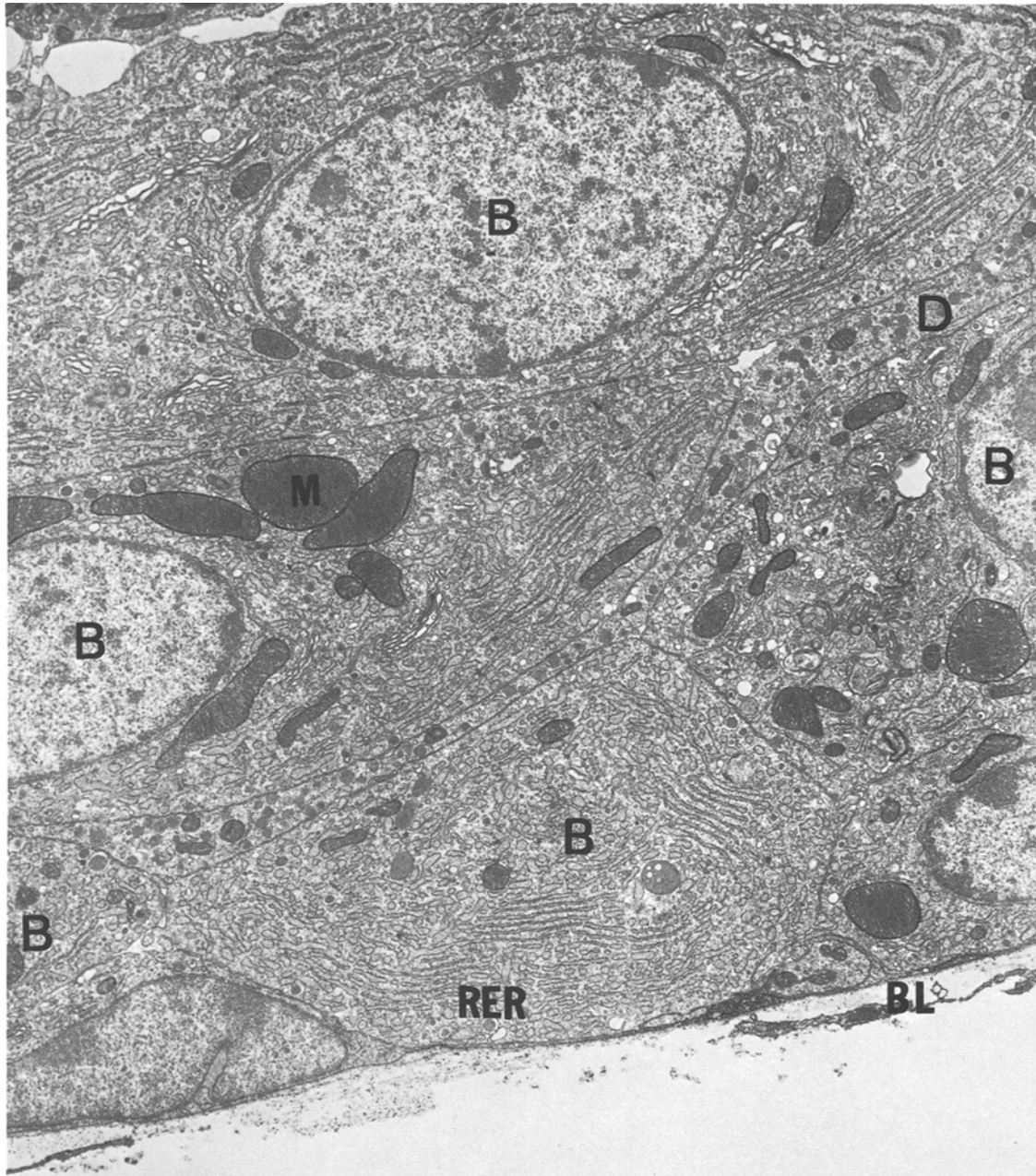
Fig. 4. Extensive D cell cyptoplasmic process extending parallel to the surface of an islet in a 20 week-old *db/db* islet. The process in view is in contact with portions of at least five B cells. Perfusion fixed, × 7,600

cell. The portion of the cell containing the nucleus represented the widest axis of the cell; the opposite pole was frequently observed as an attenuated filopodial extension of variable length and diameter. D cells, regardless of their location, were frequently seen to contact capillaries by means of cytoplasmic processes, and filopodial extensions from the cell were often seen to terminate adjacent to a capillary. In islets of normoglycaemic mice, D cells were inter-posed primarily between more numerous A cells in the mantle layer and the outermost zone of B cells. D cells were heavily granulated; granules were spherical or ellipsoidal with a mean diameter of 0.29μ (range $0.16–0.45 \mu$). The granule matrix material was of variable electron density and filled most of the granule space. A small electron-lucent space separated the granule contents from a vesicle membrane that often appeared ruffled and discontinuous. Scat-
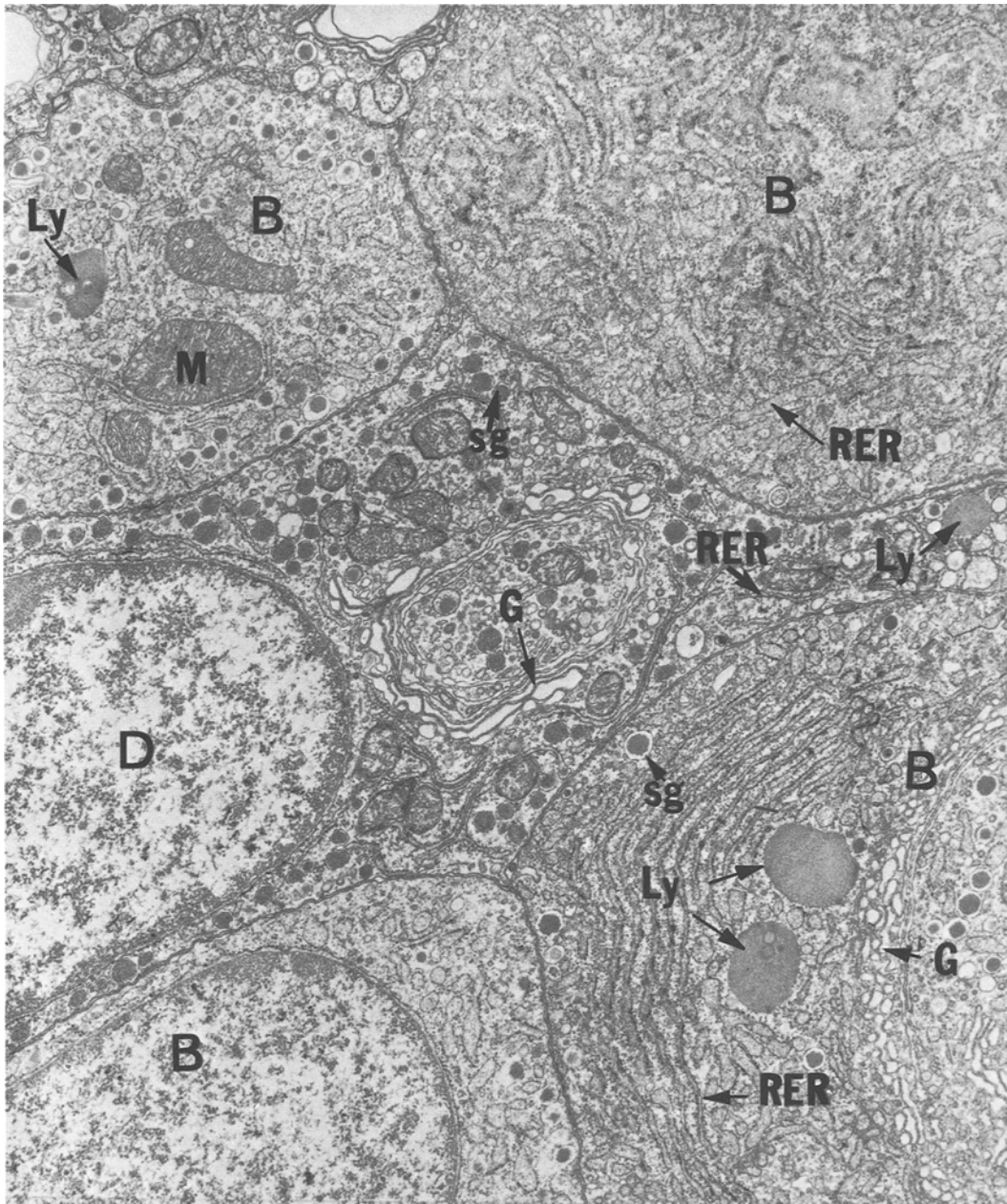
Fig. 5. The nucleated portion of a granulated D cell within the interior of the islet of a 16 week-old *db/db* mouse at the stage of advanced hyperglycaemia. The D cell is surrounded by extremely degranulated B cells, and exhibits an extensive perinuclear Golgi complex (G). Prominent lysosomes (Ly) are observed in the B cells. Collagenase isolation, × 13,000

tered profiles of rough endoplasmic reticulum (RER) and mitochondria were found throughout the cytoplasm while Golgi complexes were found mainly in the perinuclear regions. D cell surfaces were generally smooth; ciliary processes were sometimes seen. Occasional evidence of endocytosis (i. e., coated vesicle formation) and exocytosis (i. e., D granule membrane fusion with the cell membrane) was observed. Spot desmosomes were frequently seen.

In young (3 week) pre-hyperglycaemic *m db/m db* diabetes mice, no major islet ultrastructural changes from the normal other than a slight degranulation of the B cells was noted. However, with the onset of established hyperglycaemia by 7 weeks of age, the presence of D cell cytoplasmic processes appearing much deeper within the interior mass of B cells, and prior to major redistribution of the nucleated portion of the cell bodies was detected with
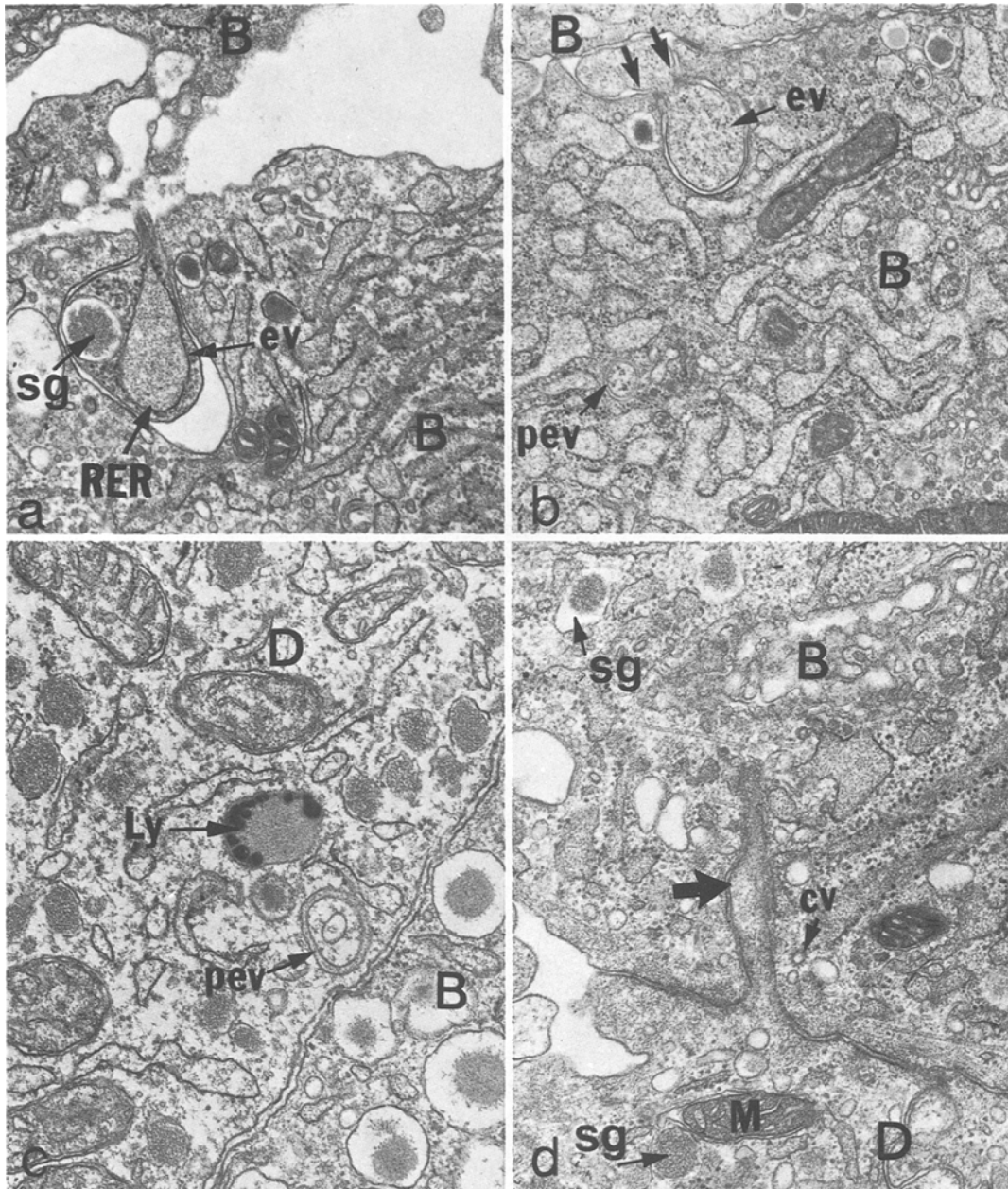
Fig. 6a–d. Cellular interactions in *db/db* islets. **a** Apparent endocytotic incorporation of a segment of B cell cytoplasm by an adjacent B cell in a 12 week-old *db/db* at the stage of advanced hyperglycaemia. Note the presence of a B granule (sg) and a profile of dilated RER inside the endocytotic vesicle (ev). Perfusion fixed, × 33,800. **b** Apparent formation of an endocytotic vesicle (ev) at the surface of a degranulated B cell in a 8 week-old *db/db* mouse. Note the points of constriction (thin arrow) where the plasma membrane appears to be enclosing the cytoplasmic projection. Note the presence of a presumed endocytotic vesicle (pev, thick arrow) inside the B cell. Collagenase isolation, × 16,600. **c** Presumed endocytotic vesicle (pev) adjacent to the plasma membrane of a D cell in a 7 week-old *db/db* mouse. A secondary lysosome (Ly) is seen nearby. Collagenase isolation, × 33,500. **d** A cytoplasmic extension (large arrow) of a D cell invaginating into the surface of an adjacent B cell in a 28 day-old *db/db* mouse. No evidence of endocytosis of the invaginated process is seen. Perfusion fixed, × 29,200

increasing frequency (Fig. 3). This intercalation of granulated, dendrite-like D cell filopodial extensions between masses of B cells was clearly evident by the time hyperglycaemia was fully established (8–9 weeks onward). The D cell extensions not only pene-

trated inward, but also extended for considerable distances parallel to the islet perimeter (Fig. 4). In mutants older than 9 weeks, nucleated D cell bodies, as well as filopodia, began to appear within the islet interior (Fig. 5) with increasing frequency such that
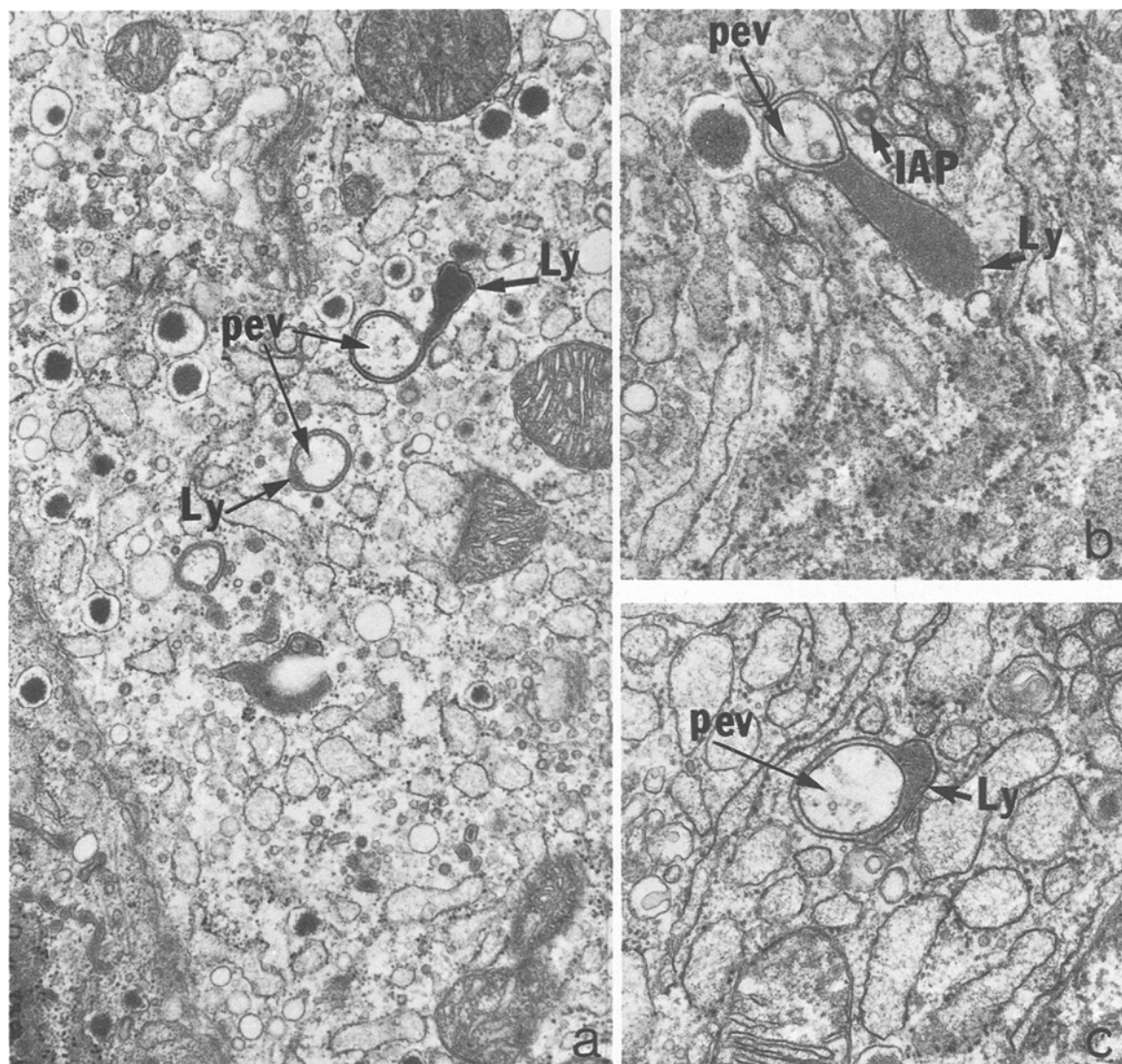
Fig. 7 a–c. Examples of apparent fusions of lysosome-like structures (Ly) that resemble primary lysosomes with presumed endocytotic vesicles (pev) in the cytoplasm of *db/db* B cells in islets of mice with advanced hyperglycaemia. An intracisternal A particle (IAP) is seen in Fig. 7 b. Collagenase isolated, **a** × 23,900, **b** × 21,200, **c** × 21,200

an obvious increase in the B cell to D cell surfaces in contact with each other was realized.

Most of the B cells seen from 7 weeks of age onward evinced the marked morphological changes characteristic of a hypersecretory state, namely, B degranulation, proliferation of tubular RER and Golgi elements, and distension of RER profiles by an electron-dense material (Figs. 3–5). The inward penetration by D cell filopodia into the B cell core prior to major redistribution of nucleated D cell bodies was not observed to be accompanied by a similar extension of A or PP cells. Further, very few morphological signs of B cell necrosis were evident when the topographical changes in the D cell population were first detected; on the contrary, as assessed

by the increased sizes of the islets isolated from 7–16 week-old mice, these changes were occurring during the phase of B cell hypertrophy and moderate hyperplasia.

With increasing severity of hyperglycaemia in the diabetic mutant from 21 days of age onward, both the hypersecretory B cells and the D cells exhibited ultrastructural surface changes. In addition to formation of coated vesicles at the cell surface, an apparent endocytotic engulfment of small portions of adjacent cells was observed (Figs. 6a and b). This phagocytotic behaviour was observed in both perfusion-fixed, hand-microdissected islets (Fig. 6a), as well as in collagenase-isolated preparations (Fig. 6b) indicating that it was not an artifact induced by enzymatic treat-

Table 1. Morphometric analysis of control and diabetic islets

Age	Genotype	N^a	Islet volume ($\mu^3 \times 10^6$)	D cell volume ($\mu^3 \times 10^5$)	D cell volume density[b]	D cells per islet	D cell particles per section
8–10 wk	+/+,+/*db*	3,30	2.13±0.25[c]	0.72±0.11	0.0343±0.0025	56.4± 6.8	9.6±0.7
	db/db	3,30	6.46±0.66	1.58±0.19	0.0251±0.0022	88.0± 7.6	15.1±1.1
	P value[d]		<0.00001	<0.00001	0.00350	0.00164	0.00005
14 wk	+/*db*	2,21	2.97±0.36	1.28±0.18	0.0424±0.0037	71.2± 8.6	13.7±1.2
	db/db	2,20	7.19±1.12	3.40±0.56	0.0480±0.0024	173.6±20.9	28.4±2.0
	P value		0.00042	0.00044	0.10971	0.00003	<0.00001
20 wk	+/+	2,20	2.06±0.35	0.77±0.16	0.0379±0.0055	54.1±9.4	11.0±1.3
	db/db	4,40	2.34±0.31[e]	1.50±0.17	0.0733±0.0043	91.2±9.5	14.8±1.1
	P value		0.28877	0.00401	<0.00001	0.00871	0.01891

[a] N = number of animals followed by the total number of islets analyzed

[b] Volume density $= \dfrac{\text{D cell volume}}{\text{Islet volume}}$

[c] Values represent mean ± SEM

[d] Student's t-test

[e] Intra-islet duct volumes not included in these measurements
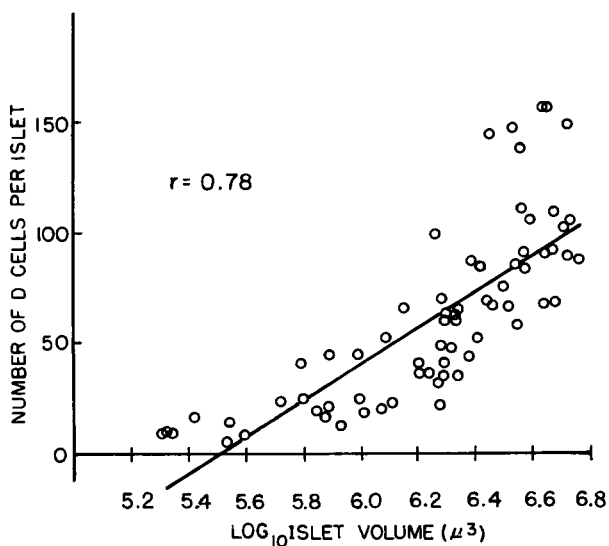

Fig. 8. Regression of D cell number per islet on islet volume ($\log_{10}$) for control islets pooled from all age groups analysed in this study. $Y = -451.3 + 81.9\times$. ANOVA for regression line: $F_{1,69} = 105.8$, $p < 0.001$

ment. En face sections through B and D cells sometimes revealed what appeared as intracellular vesicular bodies distinct from multivesicular bodies in that they were surrounded by a double unit membrane (Fig. 6c). They were usually situated close to the plasma membrane, and in some cases may well have represented microvillous projections from one cell invaginating into, but not through, the surface of an adjacent cell. Thus, the tip of the D cell pseudopod protruding against an adjacent B cell as seen in longitudinal section in Fig. 6d, if viewed in cross section,

might appear to be internalized inside the B cell. However, the frequent observation of a fusion of such double membrane-bound vesicles with single membrane-bound dense bodies that resemble primary lysosomes suggests that these structures are truly internalized and possibly catabolized via a lysosomal degradation (Figs. 7a–c).

Morphometric Analysis

Table 1 presents data from morphometric analysis of islets from control and diabetic mice of various ages. These data show that mean islet volume, D cell volume, D cells per islet, and D cell particles per section are all increased over controls in the islets of the 8 to 10 and 14 week diabetic animals with the highest values observed at 14 weeks. In the 20 week diabetic animals, however, these variables were lower than at 14 weeks. Nevertheless, they were still significantly above control values, except for the islet volume (intra-islet ductular space not included in the analysis) which was not significantly different from control values. Despite the absolute increases in mean number of D cells per mutant islet observed in all three age groups, D cell volume density exhibited a decrease in the 8 to 10 week age group of diabetics, no difference from age-matched controls in the 14 week group, and a 2-fold increase in the 20 week diabetic group. Correlation and regression analysis of the number of D cells per islet versus log islet volume for the 71 control islets analyzed in this study (Fig. 8) showed a significant positive correlation (r = 0.78, p < 0.001) between islet volume and D cell number. However, use of the calculated regression line for

control islets from all three age groups to predict D cell numbers for islets in the 8 to 10 week mutants tended to overestimate (20 out of 30) by up to 2 to 3-fold the observed values. Conversely, prediction of D cell numbers for islets from the 14 and 20 week mutants resulted in a near complete underestimation (20 out of 20 and 38 out of 40, respectively) of up to 2- to 3-fold.

Discussion

In a previous study by Baetens et al. [2], an increase in the volume density of D cells in late stage BL/Ks-*db/db* animals was observed but the method of morphometric analysis did not permit measurement of the actual numbers of D-cells. In the present study, a section by section analysis of individual islets rather than point counting [2] or linear scanning [21] methods was selected since it permitted determination of actual numbers of D cells, an estimate of D cell cytoplasmic dispersion (particles/section), and an accurate measurement of total D cell and total islet volume. Our data indicate that in animals which have made a transition from early stages of the disease when B cell hypertrophy and hyperplasia are manifest (after 5 to 6 weeks), to the stage of advanced hyperglycaemia when B cell necrosis was occurring (20 weeks and older), the mean number of D cells per islet actually increased. Thus, the observed increase in volume density is attributable to an absolute increase in the number of D cells as well as to decrease of islet size due to B cell loss.

Actual D cell volume density measurements reported here for control or *db/db* BL/Ks islets are somewhat lower than corresponding measurements for 6–12 month animals [2]. Nevertheless, the approximate 2-fold increase in volume density over controls for the 20 week *db/db* animals is similar to the 2- to 2.5-fold increase reported for 6–12 month BL/Ks diabetic mice [2], diabetic humans [27], or 14 month alloxan-diabetic rats [21], but somewhat lower than the 5.5-fold increase seen in 16 month streptozotocin-diabetic rats [27].

Of the individual mice studied, all diabetic mice in the 14 and 20 week age groups uniformly exhibited elevated mean numbers of D cells per islet. However, in the 8 to 10 week age group, only two out of three mutant mice showed mean numbers of D cells per islet that were statistically significantly increased over controls. The one 8 to 10 week mutant without a significantly increased number of nucleated D cells per islet exhibited both topographical perturbation of D cells and increased D cell particles per islet section. This indicates that positional

changes occur prior to and may be independent of D cell hyperplasia. Furthermore, initiation of D cell hyperplasia in diabetes mice appears to be secondary to B cell hypertrophy and hyperplasia which commence several weeks earlier [18]. This proliferation of D cells may be a slower response to the same diabetogenic stress(es) that leads initially to increased B cell mass, or may be a compensatory manoeuvre to restore normal volume density following B cell hyperplasia, or both.

That 8 to 10 weeks was a transitional period in D cell population change was suggested by the regression analysis for D cell number versus islet size in normal mice (Fig. 8). Extrapolation from this normal curve served to predict correctly the observed numbers of D cells per islet in only 10 of 30 mutant islets analyzed in this age group. In the other 20 islets, the extrapolated values overestimated observed values. Thus, while D cell proliferation appears to be coordinated with islet growth in normal mice, it apparently becomes uncoupled during rapid islet (B cell) growth characteristic of the young diabetic mouse. In diabetic mice in the 14 week age group, the observed number of D cells per islet had exceeded predicted values derived from the regression curve for 20 of 20 islet analyzed. This increase in D cells in the 14 week diabetic islets indicates that D cell proliferation remains uncoupled. This may imply a continued paracrine effort to control B cell hypersecretory activity by continued D cell proliferation and by increased D to B cell interaction as documented by the ultrastructural findings of this study. The increase in D cell population size, however, does not appear to be maintained indefinitely since the D cell numbers and mass attained by 20 weeks, although still significantly increased over controls, are lower than those observed at 14 weeks. This might suggest that some D cells are lost during the phase of terminal hyperglycaemia and islet degeneration. Any apparent D cell loss notwithstanding, our quantitative studies confirm that atrophic islets contain increased numbers of D cells as compared to control islets.

Present observations in normal islets of D cell orientation or "capping" at vascular structures further emphasize the potential importance of precise morphologic arrangements within the islet. Since arterial blood to the islets first perfuses the heterocellular mantle layer and then the B cell mass [9], subsequent breakdown of this arrangement would be potentially detrimental to intra-islet control processes dependent upon a vascular means of communication. Moreover, in BL/Ks diabetes, the loss of normal peripheral arrangement of non-beta cells is not limited to the D cells alone [2]. While the pronounced changes in morphology make the D cell shift

the most striking of the non-B cell rearrangements, it should be emphasized that A and PP cells also lose their peripheral distribution, and, hence, localization near the afferent blood supply, simultaneously with the D cells. Changes in the absolute numbers of these latter two cell types have not been quantified in this study.

Although penetration of D cell filipodia and migration of D cells were not detected by PAP staining for somatostatin until these mice entered a stage of established hyperglycaemia as well as hyperinsulinaemia (8–9 weeks), penetration of D cell filopodia could be detected at the ultrastructural level at the pre-hyperglycaemic stage (6 weeks). Hyperinsulinaemia, and by inference B cell hyperactivity, precedes hyperglycaemia in 10 day-old diabetes mice [5], and A cell hyperactivity in the presence of physiological levels of glucose (5.5 mmol/l) has been detected in vitro using pancreatic cell cultures established from 4–7 day-old pre-diabetic postnates [17]. Thus because the morphological rearrangements exhibited by the D cells is seen considerably after indication of A and B cell hypersecretory behaviour, it seems likely that the positional changes exhibited by the D cells are secondary to secretory perturbation in the A and B cell populations.

It is unlikely that hyperinsulinaemia alone could be the factor responsible for triggering the inward migration of D cells, since BL/6 *db/db* or *ob/ob* mice exhibit a hyperinsulinaemia more extreme than that exhibit by the BL/Ks-*db/db* mice [14] but without accompanying alterations in the peripheral distribution of D cells [2]. Moreover, exogenous insulin exhibits no acute effects on somatostatin release [28] while glucose stimulates both somatostatin and insulin release [15] by the perfused canine pancreas. Since the expression of the *db* gene on the BL/Ks versus the BL/6 inbred background is distinguished by the degree of hyperglycaemia attained at 8 weeks of age (severe in BL/Ks, mild in BL/6), it is conceivable that severe hyperglycaemia itself may affect directly D cell behaviour, particularly since similar perturbations in islet distribution can be demonstrated in streptozotocin-diabetic rats [27]. Freeze fracture studies of isolated rat islets incubated at various glucose concentrations have indicated that islet cells could rapidly increase the extent of tight junctional complexes formed between the islet cells in response to a hyperglycaemic challenge [23] or to pronase [26]. These observations prompted speculation that a labile opening and closing of such junctional complexes to stimulatory or inhibitory influences may be a mechanism for achieving intra-islet control of glucose homeostasis [23]. The great increase in cell-to-cell contacts observed between

hypersecretory B cells and portions of D cells in the islets of BL/Ks-*db/db* mice with established hyperglycaemia could suggest an intra-islet paracrine attempt to dampen B cell activity by pulses of somatostatin from the D cells entering the interstitial spaces and acting as a local inhibitor.

Ultrastructural observations reported herein have revealed unusual activity at the surfaces of the hypersecretory *db/db* B cells from the stage of established hyperglycaemia (blood glucose > 200 mg%) onward and indicate the potential for micropinocytotic and phagocytic sampling of interstitial space contents (including somatostatin). Further, the rarity of this apparent engulfment of apposing cell surfaces by B cells in islets isolated from normoglycaemic mice suggested that increased endocytosis was indeed correlated with the hypersecretory state of diabetic islets. The double membrane vesicular structures which were commonly observed in the cytoplasm of hypersecretory B cells may represent either microvillus invaginations of the cell surface of one cell into another (Fig. 6d), or, in some cases, may actually represent endocytosed portions of the plasma membrane and some adjacent cytoplasm of a neighbouring cell (Figs. 6a and b). In addition, single membrane-bound (lysosome-like) vesicles were often seen in the vicinity of, and sometimes apparently fusing with these structures. Fusion of endocytotic vesicles with primary lysosomes might be a means of catabolizing the contents of ingested material. It remains to be determined, however, whether bulk endocytosis in pancreatic islet cells represents a means of sampling fluctuating levels of metabolite or local regulatory peptides present in the interstitial spaces.

References

1. Alberti, K. G. M. M., Christensen, N. J., Christensen, S. E., Hansen, A. P., Iversen, J., Lundbaek, K., Seyer-Hansen, K., Ørskov, H.: Inhibition of insulin secretion by somatostatin. Lancet **1973 II**, 1299–1301
2. Baetens, D., Stefan, Y., Ravazzola, M., Malaisse-Lagae, F., Coleman, D. L., Orci, L.: Alteration of islet cell populations in spontaneously diabetic mice. Diabetes **27**, 1–7 (1978)
3. Coleman, D. L.: Obesity and diabetes: Two mutant genes causing diabetes-obesity syndromes in mice. Diabetologia **14**, 141–148 (1978)
4. Coleman, D. L., Hummel, K. P.: Studies with the mutation, diabetes, in the mouse. Diabetologia **3**, 238–248 (1967)

5. Coleman, D. L., Hummel, K. P.: Hyperinsulinemia in pre-weaning diabetes *(db)* mice. Diabetologia **10**, 607–610 (1974)
6. Dubois, M. P.: Immunoreactive somatostatin is present in discrete cells of the endocrine pancreas. Proc. Natl. Acad. Sci. USA **74**, 2140–2143 (1975)
7. Dubois, P. M., Paulin, C., Assan, R., Dubois, M. P.: Evidence for immunoreactive somatostatin in the endocrine cells of the human fetal pancreas. Nature **256**, 731–732 (1975)
8. Fujimoto, W. J., Ensinck, J. W., Williams, R. H.: Somatostatin inhibits insulin and glucagon release by monolayer cell cultures of rat endocrine pancreas. Life Sci. **15**, 1999–2004 (1974)
9. Fujita, T., Yanatori, Y., Murakami, T.: Insulo-acinar axis, its vascular basis and its functional and morphological changes caused by CCK-PZ and caerulein. In: Endocrine gut and pancreas. Fujita, T. (Ed.), pp. 347–357. Amsterdam: Elsevier 1976
10. Gerich, J. E., Lovinger, R., Grodsky, G. M.: Inhibition by somatostatin of glucagon and insulin release from the perfused rat pancreas in response to arginine, isoproterenol, and theophylline: Evidence for a peripheral effect on glucagon secretion. Endocrinology **96**, 749–754 (1975)
11. Goldsmith, P. C., Rose, J. C., Arimura, A., Ganong, W. F.: Ultrastructural localization of somatostatin in pancreatic islets of the rat. Endocrinology **97**, 1061–1064 (1975)
12. Holt, W. V., Healy, P.: The use of an image analyzer for measuring the cross-sectional area of Leydig cells in the testis of the cuis. Mikroskopie **32**, 76–80 (1976)
13. Hopkins, B. M.: A quantitative image analysis system. Opt. Eng. **15**, 236–240 (1976)
14. Hummel, K. P., Coleman, D. L., Lane, P. W.: The influence of genetic background on expression of mutations at the diabetes locus in the mouse. I. C57BL/KsJ and C57BL/6J strains. Biochem. Genet. **7**, 1–13 (1972)
15. Ipp, E., Dobbs, R., Orci, L., Vale, W., Unger, R. H.: Release of immunoreactive somatostatin from the pancreas in response to glucose, amino acids, pancreozymincholecystokinin, and tolbutamide. J. Clin. Invest. **60**, 760–765 (1977)
16. Koerker, D. J., Ruch, W., Chideckel, E., Palmer, J., Goodner, C. J., Ensinck, J., Gale, C. C.: Somatostatin: hypothalamic inhibitor of the endocrine pancreas. Science **184**, 482–484 (1974)
17. Leiter, E. H., Coleman, D. L., Eppig, J. J.: Endocrine pancreatic cells of postnatal "diabetes" *(db)* mice in cell culture. In vitro **15**, 507–521 (1979)
18. Like, A. A., Chick, W. L.: Studies in the diabetic mutant mouse. I. Light microscopy and radioautography of pancreatic islets. Diabetologia **6**, 207–215 (1970)
19. Like, A. A., Chick, W. L.: Studies in the diabetic mutant mouse. II. Electron microscopy of pancreatic islets. Diabetologia **6**, 216–242 (1970)
20. Marco, J., Hedo, J. A., Villaneueva, M. L.: Inhibitory effect of somatostatin on human pancreatic polypeptide secretion. Life Sci. **21**, 789–792 (1977)
21. McEvoy, R. C., Hegre, O. D.: Morphometric quantitation of the pancreatic insulin-, glucagon-, and somatostatin-positive cell populations in normal and alloxan-diabetic rats. Diabetes **26**, 1140–1146 (1977)
22. Mortimer, C. H., Tunbridge, W. G. M., Carr, D., Yeomans, L., Lind, T., Coy, D. H., Bloom, S. R., Kastin, A., Mallinson, C. N., Besser, G. M., Schally, A. V., Hall, R.: Effects of growth hormone release-inhibiting hormone in circulating glucagon, insulin, and growth hormone in normal, diabetic, acromegalic, and hypopituitary patients. Lancet **1974 I**, 697–701
23. Orci, L.: The microanatomy of the islets of Langerhans. Metabolism **25** (Suppl. 1), 1303–1314 (1976)
24. Orci, L., Unger, R. H.: Hypothesis: Functional subdivisions of islets of Langerhans and possible roles of D-cells. Lancet **1975 II**, 1243–1244
25. Orci, L., Baetans, D., Dubois, M. P., Rufener, C.: Evidence for the D-cell of the pancreas secreting somatostatin. Horm. Metab. Res. **7**, 400–402 (1975)
26. Orci, L., Amherdt, M., Henquin, J. C., Lambert, A. E., Unger, R. H., Renold, A. E.: Pronase effect on pancreatic beta cell secretion and morphology. Science **180**, 647–649 (1973)
27. Orci, L., Baetens, D., Rufener, C., Amherdt, M., Ravazzola, M., Studer, P., Malaisse-Lagae, F., Unger, R. H.: Hypertrophy and hyperplasia of somatostatin-containing D-cells in diabetes. Proc. Natl. Acad. Sci. USA **73**, 1338–1342 (1976)
28. Patton, G. S., Dobbs, R., Orci, L., Vale, W., Unger, R. H.: Stimulation of pancreatic immunoreactive somatostatin (IRS) release by glucagon. Metabolism **25** (Suppl. 1), 1499 (1976)
29. Sternberger, L. A., Handy, P. H., Cuculis, J. J., Meyer, H. C.: An unlabeled antibody method of immunocytochemistry. J. Histochem. Cytochem. **18**, 315–340 (1970)
30. Turcot-Lemay, L., Lemay, A., Lacy, P. E.: Somatostatin inhibition of insulin release from freshly isolated and organ cultured rat islets of Langerhans in vitro. Biochem. Biophys. Res. Commun. **63**, 1130–1138 (1975)

Dr. E. H. Leiter
The Jackson Laboratory
Bar Harbor, ME 04609
USA